BUTTERWORTH HEINEMANN

Polymer Vol. 36 No. 8, pp. 1559–1567, 1995

0032-3861/95/$10.00 + 0.00

An X-ray photoelectron spectroscopy surface study of solution-cast, immiscible, nylon-6/poly(*cis*-1,4-butadiene) blends

J. L. Angulo-Sanchez* and R. D. Short†

Laboratory of Surface and Interface Analysis, University of Sheffield, Department of Engineering Materials, Sir Robert Hadfield Building, Mappin Street, Sheffield S1 4DU, UK
(Received 23 June 1994; revised 3 October 1994)

In this work the surface composition of immiscible blends of nylon-6/poly(*cis*-1,4-butadiene) cast from solution have been studied by X-ray photoelectron spectroscopy. First, a mixture of two solvents capable of dissolving both polymers was designed, and then the effects of the solution concentration, solvent ratio and bulk polymer ratio on the surface composition of the blends were investigated. The results are discussed in terms of a phase diagram and show that blend surface composition is determined by the combined influence of these parameters, the strongest defining which polymer enriches the surface.

(Keywords: immiscible blends; nylon/polybutadiene; surface composition)

INTRODUCTION

Polymer blends can be obtained with a range of properties depending on the chemical nature of the polymers mixed and, more precisely, on polymer A–polymer B interactions. These interactions, short- or long-range, non-directed dispersive, or specific directional, define the basic type of blend: miscible in the case of positive interactions (attractive) between the macromolecular chain segments; and immiscible in the case of negative (repulsive). In both classes, blend properties depend on the bulk composition, but in the second, properties also depend on the specific morphology of the phases, which, in turn, is affected by the mixing method.

An extensive literature (see for example refs. 1–4) describes the study of the thermodynamic and bulk physicomechanical properties of the blends, although no one general theory accounts for all systems. In contrast, a more limited literature deals with the surface characteristics of polymer blends[5–7], and theories (in support of experimental data) are scarce. Surface characteristics, nevertheless, are very important as they totally define such properties as wettability, adhesion, friction, etc. The study of surface properties, as that of the bulk, requires the control of all variables (chemical composition, molecular weights, mixing method variables, etc.) in order to make a correct interpretation. In the study of surfaces there is also the added requirement to avoid contamination from processing aids, and other additives, which could migrate to the surface and give erroneous information.

The surface chemical characterization of a number of blends has been carried out by X-ray photoelectron spectroscopy (X.p.s.)[5–7]. These studies have been performed on films cast from solution, a method that can provide surfaces near equilibrium, and on samples prepared by melt compounding. The results from these studies show that the surface composition in blends (polymer–air interface) can be very different from that of the bulk. Theoretical studies, based on a mean-field lattice calculation[8,9], predict that surface segregation is dependent on the polymer interaction parameter (χ), molecular weight and blend bulk composition. Surface enrichment by the polymer of lower surface tension is both empirically and theoretically well established[6,8]. Recent work[10] has drawn attention to the importance of molecular architecture on surface segregation.

This paper describes an X.p.s. surface study on the immiscible blend system of polar poly(ε-caprolactam) (nylon-6) and non-polar poly(*cis*-1,4-butadiene) (PB), and it forms the basis from which chemically modified systems ('compatibilized') can be later studied. The method selected for blend preparation was solution casting to prevent mechanical degradation and thermo-oxidation, as well as to minimize the amount of contamination introduced. No common solvent has been reported for PB and nylon-6 (Ny-6); hence a solvent mixture that would dissolve both had to be designed. Mixtures of *m*-cresol (*m*-C) and 1,2-dichlorobenzene (*o*-DCB) were evaluated. The solvents were selected according to their similarity in solubility parameters (δ) and their ability to dissolve one of the polymers (*m*-C, Ny-6; and *o*-DCB, PB)[11].

The effects of total polymer solution concentration, and of solvent and bulk (polymer) composition, on the

* On leave from the Centre of Applied Chemistry Research (CIQA) at Saltillo, Coahuila, Mexico
† To whom correspondence should be addressed

surface chemical composition of solution-cast films were investigated by X.p.s. The 'as-received' Ny-6 was purified in order to assess the surface activity of low-molecular-weight Ny-6 formed by 're-equilibration'. The results have been analysed looking for trends and compared with the behaviour predicted by theory. However, we note that theory describes systems that have achieved equilibrium; solution casting may not produce such systems.

THEORY

Analysis of interaction parameters and solubilities

Polymer solubility, and solvent–solvent or polymer–polymer miscibility, can be looked at in terms of thermodynamic parameters; perhaps the most widely used is the interaction parameter (χ). The polymer–solvent or polymer–polymer interaction parameter is defined in the Flory–Huggins (FH) theory as:

$$\chi = \frac{V_r(\delta_1 - \delta_2)}{RT} \tag{1}$$

with χ = interaction parameter, V_r = volume of reference (generally molar volume), δ_i = solubility parameter, R = gas constant, and T = absolute temperature. A χ value of less than 0.5 is generally taken as indicative of total solubility over the complete range of composition.

The solubility parameter is defined by:

$$\delta_i = \left(\frac{\Delta E_i^v}{V_i}\right)^{1/2} \tag{2}$$

where ΔE_i^v = energy change upon isothermal vaporization of the saturated liquid to the ideal gas state, at infinite volume, or cohesive energy density (CED), and V_i = molar volume of the species i. The energy change ΔE_i^v is related to the enthalpy of vaporization:

$$\Delta E_i^v = \Delta H_i^v - RT \tag{3}$$

and, for solvents, it can be determined by measuring the enthalpy of vaporization or a correlation for ΔH_i^v.

In the case of polar systems, Hansen[12] and Hansen and Skaarup[13] assume that the cohesive energy arises from the dispersive, permanent dipole–dipole interactions and hydrogen-bonding forces, and they report the equation:

$$\delta^2 = \delta_D^2 + \delta_P^2 + \delta_H^2 \tag{4}$$

where δ_D^2 is the dispersive term, δ_P^2 the polar term and δ_H^2 the hydrogen-bonding term. The solubility parameters obtained with equation (4) give better agreement, with experimental data, than those obtained with equation (2), but still they are not always accurate in predicting the solution thermodynamics for every system.

Coleman[14] has reported a series of group molar attraction (F) and molar volume constants (V^*) from which it is possible to calculate the solubility parameter of any polymer, as long as the repeat unit is known:

$$\delta = \sum(F/V^*) \tag{5}$$

Coleman's values are selected later to make predictions on solvent–solvent and polymer–solvent miscibility. In the case of polymer–polymer miscibility, the critical value of the interaction parameter (χ_{crit}) defines the limit of solubility[14] and is a function of the degree of polymerization (x_i):

$$\chi_{crit} = (\tfrac{1}{2})(1/x_A^{1/2} + 1/x_B^{1/2})^2 \tag{6}$$

The above equations have been applied in this work, to evaluate the solubility of the polymers and solvents used in blend preparation.

Surface composition

Theoretical calculations and experimental results show that the surface composition of polymer blends may be very different from that of the bulk, and that a number of factors control surface segregation. The mean-field calculations of Kumar[8,9], for athermally mixed polymers, which interact through short-range dispersive forces, predict that surface segregation is affected by molecular weight, differences in polymer chemical structure and blend bulk composition. The model used predicts that only minor surface enrichments (less than 1%) are expected to arise from (purely) molecular-weight differences. From this it follows that changes in polymer chemical structure and blend composition have a much more profound influence, promoting a significant surface enrichment of one of the polymers. The results of calculations show that the component of lower surface energy (a direct property of polymer chemical structure) segregates to the surface, the driving force for this partitioning arising from even very small differences in surface energy. Calculation also reveals that this segregation ought to be most marked when the weight fraction (of the low-surface-energy component) is low. However, more recent work by Hariharan[10] with mixtures of deuterated and protonated polystyrene of equal and disparate molecular weights has shown that either component could partition to the surface, depending on the specific combinations of molecular weight employed. The results highlight the fact that chain length has an importance above that predicted by the mean-field lattice calculation used earlier. This draws attention to 'compressibility' in modelling polymer blends near surfaces[10].

Bonn and van Aartsen[15] have suggested that the solubility parameter (δ) and surface tension (γ) of a polymer can be correlated through the empirical equation:

$$\delta \propto \gamma^{1/2}(1/\text{area})^{1/4} \tag{7}$$

where the area corresponds to that of the polymer segment surface. Although this relationship has been superseded by more sophisticated expressions for γ (see equation (19) in ref. 16), using equation (7) simply as a predictive guide, we would expect in our system that Ny-6 (higher δ and area) has the greater γ. Values of critical surface tension of 31 mN m^{-1} for PB[17] and 38 mN m^{-1} for Ny-6[18] have been reported. Hence, the surface tension argument predicts that at equilibrium in Ny-6/PB blends some PB will have segregated to the surface.

Surface characterization

Surface composition and concentration–depth profiles in polymer blends have been studied by X.p.s. The analysis depth of this technique is related to the take-off angles (TOA) with respect to the sample surface (θ), and is calculated through the equation[19]:

$$d = \lambda \sin\theta \tag{8}$$

where λ is the inelastic mean free path of the electrons,

reported to be equal to 1.5 nm for C 1s electrons when using Mg Kα X-rays[20]. Quantitative analysis is carried out using the integrated peak areas of characteristic elements for each polymer. The repeat units for Ny-6 and PB are:

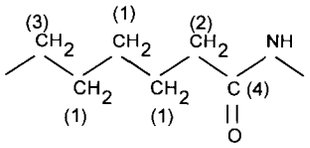

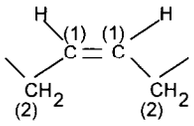

respectively. For composition calculations we used the nitrogen percentage measured for the blend $\%N_{1s,b}$ and for nylon homopolymer $\%N_{1s,Ny}$, to calculate the surface nylong weight fraction ($W_{Ny,s}$) through:

$$W_{Ny,s} = \frac{\%N_{1s,b}}{\%N_{1s,Ny}} \tag{9}$$

The Ny-6 weight fraction in the Ny-6/PB system can be written as:

$$W_{Ny} = \frac{w_{Ny}}{w_{Ny} + w_{PB}} \tag{10}$$

and that of the polybutadiene would be:

$$W_{PB} = 1 - W_{Ny} \tag{11}$$

where w_{Ny} and w_{PB} are the weight (in grams) of the polymers.

In this study, nylon segment fraction (ϕ_{Ny}) has been preferred over weight fraction because all thermodynamic properties are related to volume fraction, and to the polymer segment fraction. Segment fraction is defined by:

$$\phi_{Ny} = \frac{x_{Ny}N_{Ny}}{x_{Ny}N_{Ny} + x_{PB}N_{PB}} \tag{12}$$

where x_{Ny} = degree of polymerization and N_i = number of molecules of each polymer.

Using the definition of mole number $n_i = w_i/MW_i$ and of degree of polymerization $x_i = MW_i/m_i$, equation (12) can be transformed into an equation expressed in terms of the polymer weights w_i and the molecular weight of the repeat units m_i:

$$\phi_{Ny} = \frac{w_{Ny}/m_{Ny}}{w_{Ny}/m_{NY} + w_{PB}/m_{PB}} \tag{13}$$

Equation (10) can be rearranged to obtain the nylon weight:

$$w_{Ny} = (w_{Ny} + w_{PB})W_{Ny} \tag{14}$$

and the butadiene weight:

$$w_{PB} = (w_{Ny} + w_{PB})(1 - W_{Ny}) \tag{15}$$

By substituting equations (14) and (15) in equation (13) we obtain the nylon segment fraction:

$$\phi_{Ny} = \frac{W_{Ny}}{W_{Ny}/m_{Ny} + (1 - W_{NY})/m_{PB}} \tag{16}$$

The nylon surface segment fraction ($\phi_{Ny,s}$) may be calculated by using the value for $W_{Ny,s}$ from equation (9).

Later, we also use a parameter, the absolute surface segregation ($A_{Ny,s}$), which is given by:

$$A_{Ny,s} = \phi_{Ny,s} - \phi_{Ny,b} \tag{17}$$

EXPERIMENTAL

Materials

Polymers. Standard PB from Aldrich, with a degree of polymerization of $\bar{x}_n = 1460$, measured by size exclusion chromatography (s.e.c.), was used as received, Ny-6 with a reported value of $\bar{x}_n = 313$ from Polysciences Inc. was used in two forms: (1) 'as received' (original) Ny-6; (2) Soxhlet extracted with methanol to remove any monomer or cyclic oligomers[21] that might be present in the polymer; this material is referred to as 'purified' Ny-6.

Solvents. *m*-Cresol (*m*-C) (>99% pure) and 1,2-dichlorobenzene (*o*-DCB), h.p.l.c. grade, from Aldrich were used as solvents for Ny-6 and PB respectively. Tetrahydrofuran (THF), h.p.l.c. grade, was used as carrier solvent for PB molecular-weight measurements, and chloroform, h.p.l.c. grade, was used for nylon.

Molecular-weight determinations

Molecular-weight distribution and averages of PB were determined in a GPC-150C Waters chromatograph with refractive index detector, and three Microstyragel analytical columns (25 cm length), two with nominal porosity of 10^6, 10^4 (Å) and one of mixed porosity. THF was used as carrier solvent at 30°C and with a 1 ml min^{-1} flow rate. Calculations of molecular-weight averages were done using a universal calibration curve constructed with polystyrene standards and the Mark-Houwink constants reported[22] for PB.

The nylon was analysed by first derivatizing the polymer (*N*-trifluoroacetylation)[23], and later running it in chloroform at 30°C, with a 1 ml min^{-1} flow rate[22]; the chromatograph was equipped with a u.v. detector.

The phase diagram

To produce the phase diagram by the solvent–non-solvent method, solutions with different initial polymer concentrations and polymer ratio, and of different solvent compositions, were prepared. These were placed in a thermostated cell with stirring, and later one solvent was added dropwise until the cloud point was reached; at this point the solvent composition and solution concentration were determined. For the low *m*-C points, the starting solution was in the two-phase region and *m*-C was added until the turbidity in the solution disappeared.

Blend preparation

Two series of blends were prepared: series A, keeping the bulk composition fixed at $\phi_{Ny} = 0.32$, but changing the solution concentration and solvent composition; and series B, where the solvent ($X_{m\text{-}C} = 0.5$) and solution concentration (5 and 10 g l^{-1}) were fixed and the polymer ratio (Ny-6/PB) varied from 0/100% to 100/0% in 10% increments. Series B samples were prepared with original and purified Ny-6.

Series A. Five solvent mixtures (*m*–C/*o*-DCB) with *m*-C mole fraction ($X_{m\text{-}C}$) of 0.15, 0.30, 0.40, 0.50 and 0.60,

Table 1 Solubility parameters of polymers and solvents: experimental and calculated

Substance	$\delta((\text{cal cm}^{-3})^{1/2})$		
	Obs.	Hansen	Coleman
m-Cresol	10.2[a]	11.09[a]	10.1[c]
o-Dichlorobenzene	10.1[a]	10.02[a]	11.1[c]
Poly(*cis*-1,4-butadiene)	8.4–8.6[a]	9.23[b]	8.1[c]
Nylon-6	–	–	10.5[c]

[a] Ref. 10
[b] Ref. 4, p. 54
[c] Equation (5) with constants from ref. 14

were used for polymer solution blending and film casting. Different amounts of Ny-6 were placed in the *m*-C/*o*-DCB mixtures and heated to 80°C, with occasional shaking, for dissolution; afterwards PB was added (to obtain a final Ny-6 bulk segment fraction concentration ($\phi_{Ny,b}$) of 0.32. This was left overnight for dissolution. Alternatively, and less time-consuming, Ny-6 was dissolved in *m*-C and PB in *o*-DCB, at their final concentration, then both solutions were mixed. Solubility was assessed visually by the absence of solid residues. Films prepared from solutions with polymer concentrations in the range 1 to 30 g l^{-1} were evaluated.

Series B. Samples in series B were prepared using the same method.

Film preparation

Blend solutions were placed in aluminium pans (4 cm diameter) and the solvents vacuum evaporated at 85°C; this temperature is higher than the polymer glass transitions of PB (−102°C) and Ny-6 (62°C). From the resultant films, samples for surface analysis were obtained; only the air-facing surfaces were analysed.

Surface characterization of the blends

X.p.s. studies were carried out on a VG CLAM 200 photoelectron spectrometer from VG (Microtech Ltd), using non-monochromated Mg Kα X-rays from the dual-anode source for excitation. The X-ray source was operated at 10 kV and 10 mA; the analyser was operated in fixed analyser transmission (FAT) mode with a pass energy of 100 eV for wide scans and 20 eV for narrow scans. The pressure in the system was maintained around 1×10^{-8} Torr. A wide scan (obtained by adding four runs), as well as carbon (C1s), nitrogen (N 1s) and oxygen (O 1s) core lines, were recorded for each sample. The results were used to determine whether there was any surface segregation under the conditions used to prepare the blends; analysis of the homopolymers was also carried out. A minimum of three samples were analysed at each composition. Data presented in figures correspond to the average value.

RESULTS AND DISCUSSION

Solubility behaviour

Measured and calculated solubility parameters are quoted in *Table 1*. We were unable to find an experimentally determined solubility parameter for Ny-6, and have, therefore, chosen to use values calculated using the approach of Coleman[14]. These values are given in the third column of this table and the interaction parameters χ_{AB} were calculated by means of equation (1), using the solvent molar volume as V_r. The results are shown in *Table 2*, and are used to discuss the solubility behaviour of polymers and solvents.

First, we consider *m*-C with the other solvent and the polymers:

(a) The interaction parameter (0.16 using $V_r = V_{m\text{-C}}$) for mixing with *o*-DCB is lower than the critical value (0.5). Hence miscibility in the whole composition range is predicted. Experimental results agree with this prediction.

(b) For Ny-6 in *m*-C, the interaction parameter (0.026) is lower than the 0.5 limit and solubility of the polymer is predicted, in agreement with the reported behaviour and experimental results.

(c) For PB with *m*-C, the calculated χ_{AB} value (0.65) predicts insolubility, in agreement with our experimental results.

Secondly, we consider *o*-DCB:

(d) The interaction parameter for the solvent pair is low, 0.18 (using $V_r = V_{o\text{-DCB}}$), again, predicting miscibility.

(e) For Ny-6 in *o*-DCB, the interaction parameter (0.065) is similar to that obtained in (b) and predicts solubility of the polymer. However, experimentally, no apparent dissolution was observed. We note that Ny-6 and *m*-C interact through hydrogen bonding and presume that these interactions are not possible in the Ny-6/*o*-DCB pair. Therefore, despite a low interaction parameter, the strong hydrogen bonding in the Ny-6 renders the polymer insoluble in *o*-DCB.*

(f) The calculated interaction parameter for PB in *o*-DCB (1.62) is well above the 0.5 limit, hence insolubility is predicted; however, *o*-DCB is reported as a solvent for PB[11] and the polymer was easily dissolved, even at the relatively high concentration of 15 g l^{-1}. It has been reported that chlorinated solvents can associate through Lewis acid–base interactions[24] and that the solubility parameter range is extended when this intereaction takes place between a polymer and solvent[25]; the solubility of PB may be related to this type of process. The insolubility of Ny-6 in *o*-DCB would support this assumption.

Finally, the polymer–polymer system has a very low critical value (3.5×10^{-3}) due to the polymers' high molecular weight, and immiscibility is predicted. The interaction parameter values (0.59 when taking V_{PB} as the reference volume, and 0.99 when using V_{Ny}) is much higher than the critical value. The immiscible behaviour of this blend has been reported[26].

Table 2 Predictions of miscibility based on solubility parameters: interaction parameters calculated using equation (1) and Coleman values

Substance	*m*-C	*o*-DCB	PB	Ny-6
m-Cresol	–	0.18		
o-Dichlorobenzene	0.16	–		
Poly(*cis*-1,4-butadiene)	0.65	1.62	–	
Nylon-6	0.026	0.065	0.45	–

* Had we chosen the Hansen or experimental value for δ(*o*-DCB) we would still have predicted miscibility

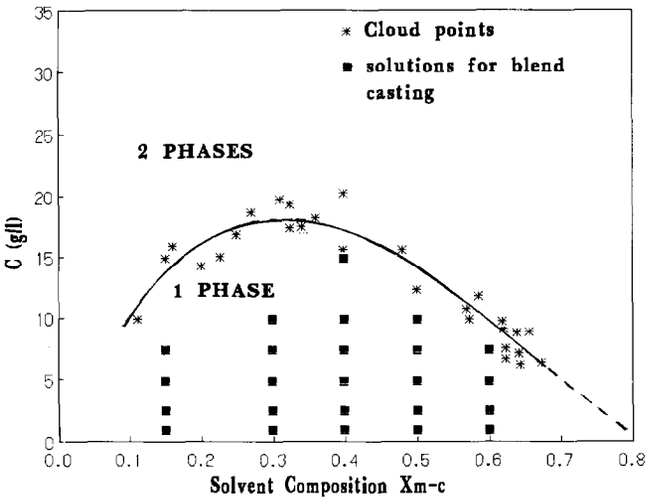

Figure 1 Phase diagram for PB and Ny-6 in *m*-C and *o*-DCB solvent ($X_{m\text{-}C}=0.0$–1.0)

The divergence between the predicted behaviour and observed behaviour (in (e) and (f)) highlights the importance of specific directional bonding, something that cannot be accounted for when using solubility parameters. In conclusion, we can say that: the solvents are miscible, *m*-C is a solvent for Ny-6, *o*-DCB for PB, but the solvent for a given polymer behaves as a non-solvent for the other polymer. This behaviour was used to dissolve both polymers and prepare the blends in mixtures of these solvents; as well as to construct the phase diagram for the system.

The phase diagram

Because the solvent for one individual polymer behaves as a non-solvent for the other, high concentrations of that particular solvent will promote the dissolution of one polymer, but the precipitation of the other. The phase-separation curve for different solvent compositions and (total) polymer concentrations was obtained by determination of the cloud point (*Figure 1*). This figure shows that mixtures with a $X_{m\text{-}C}$ mcle fraction above 0.8 will promote phase separation, even at very low polymer concentration. The point at which polymer precipitated on the low *m*-C concentration side proved very difficult to determine, as there was no noticeable change in solution turbidity with precipitation. Hence, the exact position of the phase-separation curve is unknown in this region, and it is quite likely that the phase-separation boundary lies within the curve drawn. We have fitted to the data points (in which we have confidence) a third-order curve, in keeping with Tompa[27]. Addition of data points for low $X_{m\text{-}C}$ might well change the position of the curve intersection with the *x* ordinate (to a value of $X_{m\text{-}C}$ closer to 0.1) whilst remaining third order; the effect of this at high $X_{m\text{-}C}$ would be to reduce slightly the value of the *x* intersection to a point somewhere closer to 0.7. In the figure the different solutions used for blend preparation are also shown; solutions prepared with a $X_{m\text{-}C}=0.15$ are close to where we believe the phase-separation boundary to lie. The same is also true for the $7.5\,g\,l^{-1}$ blend prepared with a $X_{m\text{-}C}$ of 0.6. Later it is shown that these solutions produced blends whose surface compositions did not follow the trend observed in the other samples.

On solvent evaporation, the *o*-DCB (b.p. = 179–180°C) will evaporate faster than *m*-C (b.p. = 202°C), so any given point inside the one-phase zone will tend to move upwards and to the right side of the diagram, crossing over the phase-separation line and eventually becoming dry. As we will show, different surface compositions may be attained depending on the 'starting point' of the original solution in the diagram.

Surface characterization

The surface %N was obtained by taking the number of counts under the N 1s and C 1s core levels, ratioing and multiplying by the sensitivity factors appropriate for the instrument on which the spectra were obtained. From the %N the surface segment fraction was calculated using the procedure outlined earlier.

Series A: blends with fixed bulk composition in different solvents and concentrations

The measured $\phi_{Ny,s}$ for samples cast from polymer/solvent mixes of different solvent compositions and total polymer concentrations are displayed in *Table 3*. Where the values quoted are the average of at least three measurements, the standard deviation (*SD*) is also given. In *Figure 2*, $\phi_{Ny,s}$ is plotted *versus* X.p.s. sampling depth for polymer solution concentrations ranging from 1 to $30\,g\,l^{-1}$ (solvent composition fixed at $X_{m\text{-}C}=0.5$ and $\phi_{Ny,b}=0.32$). The data reveal the following:

(i) A slight variation in the Ny-6 concentration through the sampling depth, i.e. a small depletion of Ny-6 at the very surface. However, such depletion, within the limits of experimental error of the X.p.s. analysis (±5%), is not significant. In the Ny-6 homopolymer, where traces of siloxane were detected, a similar concentration profile was noted, and in general it can be said that there was no nitrogen profile in the homopolymer of these blends

(ii) There is a very strong solution concentration effect. All samples were prepared with a fixed Ny-6 segment fraction ($\phi_{Ny,b}=0.32$); however, blends were produced with very different surface segment fractions ($\phi_{Ny,s}=0.01$–0.89).

This effect is even more evident in *Figure 3* where $\phi_{Ny,s}$ has been plotted against starting solution concentration

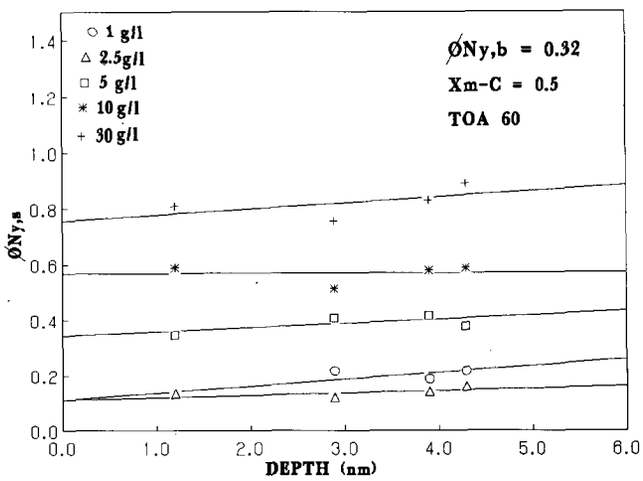

Figure 2 $\phi_{Ny,s}$ as a function of X.p.s. sampling depth ($\phi_{Ny,b}=0.32$, $X_{m\text{-}C}=0.5$)

Table 3 Ny-6 surface segment fraction ($\phi_{Ny,s}$) for constant composition blends ($\phi_{Ny,s}=0.32$) cast from different solvent mixtures and solution concentrations[a]

$X_{m\text{-}C}$	D (nm)	$C=1.0\,g\,l^{-1}$		$C=2.5\,g\,l^{-1}$		$C=5.0\,g\,l^{-1}$		$C=7.5\,g\,l^{-1}$		$C=10.0\,g\,l^{-1}$		$C=30.0\,g\,l^{-1}$	
		ϕ_{Ny}	SD	ϕ_{Ny}	SD	ϕ_{Ny}	SD	ϕ_{Ny}	SD	ϕ_{NY}	SD	ϕ_{Ny}	SD
0.15	1.2	0.23	0.06	0.07	–	s.c.	–	0.09	–	n.p.	–	n.p.	–
	2.0	0.26	0.09	0.08	–	s.c.	–	0.10	–	n.p.	–	n.p.	–
	3.9	0.25	0.06	0.10	0.05	n.p.	n.p.	0.12	0.08	n.p.	–	n.p.	–
	4.3	0.25	0.07	0.12	–	n.p.	n.p.	0.10	–	n.p.	–	n.p.	–
0.30	1.2	0.11	0.16	0.03	–	0.14	–	s.c.	–	0.67	0.09	n.p.	–
	2.9	0.14	0.14	0.04	–	0.15	–	s.c.	–	0.67	0.08	n.p.	–
	3.9	0.15	0.18	0.08	0.06	n.p.	n.p.	s.c.	–	0.78	0.08	n.p.	–
	4.3	0.15	0.18	0.04	–	n.p.	n.p.	s.c.	–	0.81	0.17	n.p.	0
0.40	3.9	0.11	0.13	0.24	0.05	0.33	0.11	0.64	0.06	0.73	0.06	0.88[b]	0.06[b]
0.50	1.2	0.13	0.04	0.13	–	0.35	0.07	0.35	–	0.59	0.36	0.81	–
	2.9	0.22	0.06	0.12	–	0.41	0.08	0.40	–	0.52	0.19	0.76	–
	3.9	0.19	0.06	0.14	0.03	0.42	0.02	0.49	0.10	0.58	0.21	0.83	0.1
	4.3	0.22	0.05	0.16	–	0.38	0.11	0.51	–	0.59	0.23	0.89	–
0.60	1.2	0.16	–	0.01	–	0.26	–	0.29	–	n.p.	–	n.p.	–
	2.9	0.13	–	0.02	–	0.25	–	0.40	–	n.p.	–	n.p.	–
	3.9	0.13	0.02	0.02	0.02	0.24	0.06	0.30	0.02	n.p.	–	n.p.	–
	4.2	0.15	–	0.02	–	0.27	–	–	–	n.p.	–	n.p.	–

[a] SD = standard deviation
s.c. = samples with solvent residues
n.p. = not prepared samples
[b] Concentration $15\,g\,l^{-1}$

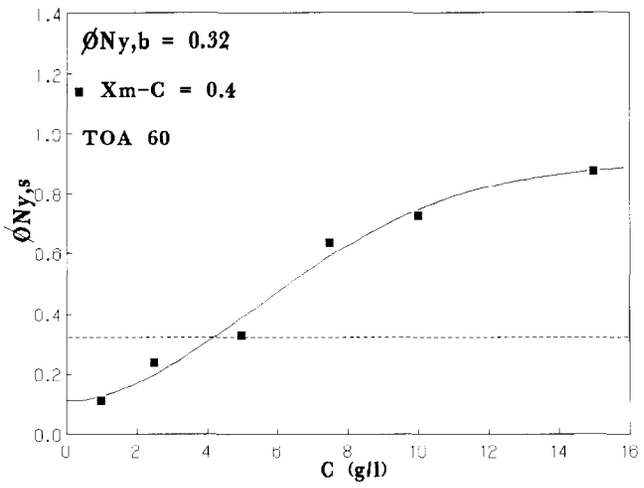

Figure 3 Effect of (total polymer) solution concentration on $\phi_{Ny,s}$ ($\phi_{Ny,b}=0.32$, $X_{m\text{-}C}=0.4$)

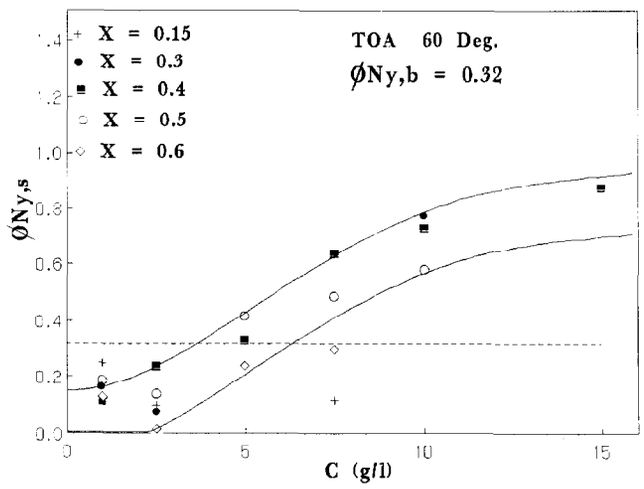

Figure 4 Effect of solvent and solution concentration on $\phi_{Ny,s}$

for blends prepared with a solvent composition of $X_{m\text{-}C}=0.4$. Here, we can see that, as the solution concentration was raised (from 1 to $15\,g\,l^{-1}$), the amount of Ny-6 at the surface of the film also increased. At low solution concentrations (less than $5\,g\,l^{-1}$) there was a Ny-6 depletion, while above this concentration Ny-6 enrichment occurred. Extrapolating this behaviour, Ny-6-only surfaces would be produced from high solution concentrations, the limit being the maximum amount of polymer that is soluble in this solvent composition (see *Figure 1*).

The above behaviour was observed in all the blends that were cast from polymer/solvent mixes, of different solvent compositions and polymer concentrations, which were safely within the one-phase region or close to the maximum polymer solubility (0.3–0.5) described in *Figure 1*. This point is illustrated in *Figure 4*, where the surface compositions determined for these blends all fall within a narrow band. Hence, it is clear that here the effect of solvent composition is not paramount. The surface compositions of blends cast from the $X_{m\text{-}C}=0.15$ solvent compositions (most polymer concentrations) and

from the $X_{m\text{-}C}=0.6$ solvent with a polymer concentration of 7.5 g l^{-1} fall outside the narrow band of data points in *Figure 4*. On inspection of *Figure 1* we can see that these points exist close to the phase-separation boundary. We believe that these polymer/solvent mixes must fall within the spinodal–binodal region, and it is for this reason that they do not behave as the others.

In *Figure 5*, the data for three solvent compositions ($X_{m\text{-}C}=0.15$, 0.4 and 0.6) have been overlaid on the phase diagram. *Figure 5* illustrates how dependent surface composition is on the 'starting position' in the one-phase region. The figure also shows how close the discussed polymer/solvent mixes were to the boundary for phase separation.

It is worth considering how well the above data correlate with the expected behaviour, based on the surface tension argument. If surface tension were to control surface enrichment, we would expect to see an enrichment of the surface with PB, irrespective of polymer solution concentration or solvent composition. Hence, these results draw attention to the fact that the surface composition is, in the main, controlled by polymer–solvent interactions.

In order to explain the behaviour in surface enrichment seen in *Figures 2–5*, it is necessary to take into account the combined effects of solvent removal rate and the initial position on the phase diagram. Considering solvent removal, we can (safely) assume that the *o*-DCB will come off faster than the *m*-C (owing to the difference in their boiling points). This has the result of reducing the solubility of the PB in the system: (i) because it is the higher-molecular-weight component; and (ii) owing to the relative increment of *m*-C, which is a non-solvent for this polymer. Hence, PB precipitates first, leaving a solution rich in Ny-6 to be precipitated later. The original concentration of the solution is important as it determines how close the system is from the phase-separation line (see *Figure 1*). As the polymer concentration is raised, the closer we move to this line, which, in principle, will favour (first) the precipitation of the higher-molecular-weight polymer (the PB). During film formation, as the solvent is removed we move to the right and upwards on the phase diagram, and when we reach the phase-separation curve PB is precipitated. At any fixed solvent composition, the greater the polymer concentration, the closer we are on *Figure 1* to the phase-separation curve, the sooner PB precipitation occurs on solvent removal. This certainly

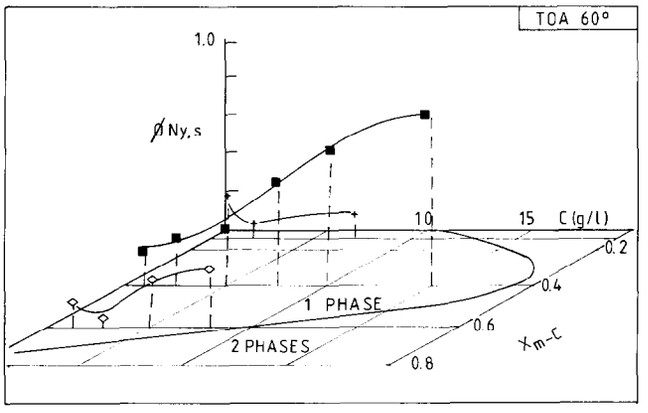

Figure 5 Overlay of selected data from *Figure 6* on the phase diagram

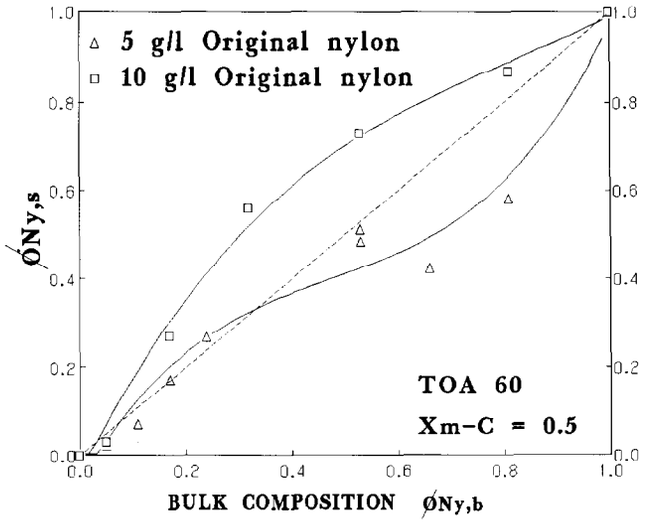

Figure 6 $\phi_{Ny,s}$ *versus* $\phi_{Ny,b}$ ($X_{m\text{-}C}=0.5$) for 'as-received' Ny-6 (5 and 10 g l^{-1})

applies to the blends prepared from solutions with $X_{m\text{-}C}=0.3$, 0.4, 0.5 and 0.6 (excluding the 7.5 g l^{-1} blend). The possible exception is the $X_{m\text{-}C}=0.15$ g l^{-1} case, where the *m*-C content (solvent for Ny-6) was very low and the solutions were already very close to or at the point of phase separation. (In this region the curve describing phase separation can only be extrapolated from other measurements, and is consequently least well known.) The data reported show this system to produce Ny-6-deficient surfaces and, therefore, we assume that the Ny-6 did not stay preferentially in solution on solvent removal.

Series B: different bulk composition blends, cast from $X_{m\text{-}C}=0.5$ *solvent mixtures*

Displayed in *Figure 6* are the surface–bulk segment fraction plots for blends prepared with the 'original' Ny-6. Two different (total) polymer concentrations were investigated (5 and 10 g l^{-1}) whilst the solvent composition was kept fixed. From the plots we can see that the $\phi_{Ny,s}$ is dependent upon $\phi_{Ny,b}$, as expected, but that the polymer solution concentration effect overrides this behaviour totally, changing $\phi_{Ny,s}$ between 5 and 10 g l^{-1}.

The tie-line indicates the point where $\phi_{Ny,s}=\phi_{Ny,b}$. In the 5 g l^{-1} system there was no preferential surface enrichment of Ny-6 at the surface at low $\phi_{Ny,b}$. However, at high $\phi_{Ny,b}$ we can see that there was Ny-6 depletion at the surface.* In the 10 g l^{-1} system there was Ny-6 surface enrichment at all $\phi_{Ny,b}$.

Before considering why the 5 g l^{-1} system behaves as seen in *Figure 6*, it is necessary to consider in more detail the presence of low-molecular-weight material (LMWM) in the Ny-6. This polymer is well known to depolymerize (re-equilibrate) to produce low-molecular-weight oligomers above its melting temperature[21]. The effect of the low-molecular-weight components on the surface composition is shown in *Figure 7* for the 5 g l^{-1} system and *Figure 8* for the 10 g l^{-1} system. *Figure 7* shows that there was an appreciable reduction of the amount of Ny-6 at the surface of the blends prepared

* We do not know the phase diagram for total polymer concentration *versus* $\phi_{Ny,b}$, and, therefore, do not have an adequate explanation for why such complex behaviour occurs

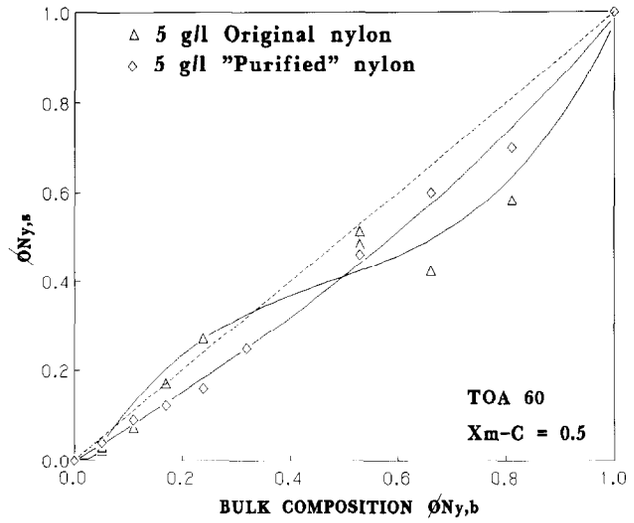

Figure 7 $\phi_{Ny,s}$ *versus* $\phi_{Ny,b}$ ($X_{m\text{-}C}=0.5$) for 'as-received' Ny-6 and purified Ny-6 ($5\,g\,l^{-1}$)

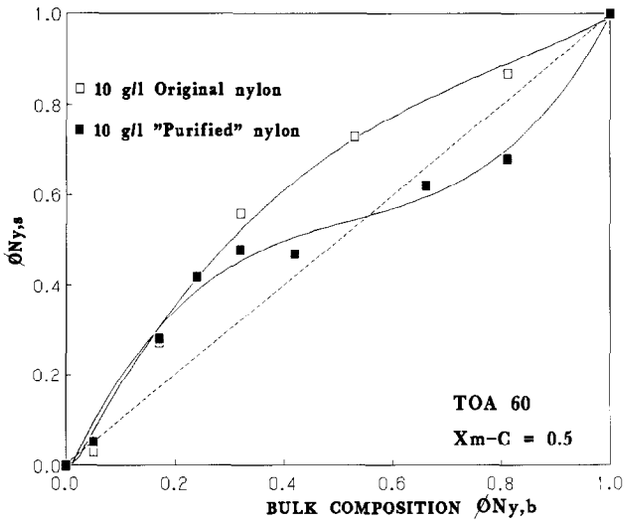

Figure 8 $\phi_{Ny,s}$ *versus* $\phi_{Ny,b}$ ($X_{m\text{-}C}=0.5$) for 'as received' Ny-6 and purified Ny-6 ($10\,g\,l^{-1}$)

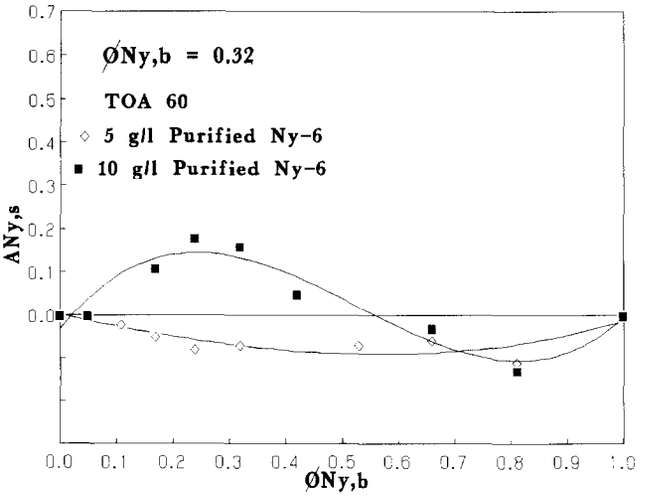

Figure 9 Absolute segregation as a function of $\phi_{Ny,b}$ for 5 and $10\,g\,l^{-1}$ purified Ny-6

with the purified Ny-6 in the low $\phi_{Ny,b}$ blends. There is, even, an apparent depletion of Ny-6 at the surface, which is predicted by the surface tension argument. This behaviour strongly suggests that any Ny-6 excess was due to LMWM. *Figure 8* reveals a similar effect in the $10\,g\,l^{-1}$ system; however, a surface excess of Ny-6, at low Ny-6 bulk concentration, is still observed. Even after Ny-6 purification, the curves for the 5 and $10\,g\,l^{-1}$ are significantly different, drawing attention to the importance of solution concentration (polymer–solvent interactions) in determining surface composition.

The difference in behaviour with $\phi_{Ny,b}$ is better shown by the plots of absolute segregation (calculated with equation (17)) in *Figure 9*. In samples cast from $5\,g\,l^{-1}$ solution concentration, there was no Ny-6 excess at the surface, but on raising the concentration to $10\,g\,l^{-1}$ there was an absolute enhancement of Ny-6 at the surface below $\phi_{Ny,b}=0.6$. Above this concentration, in both systems there was a surface depletion of Ny-6. Particularly interesting is the point at ca. $\phi_{Ny,b}=0.55$ on the $10\,g\,l^{-1}$ curve: at this point $\phi_{Ny,b}=\phi_{Ny,s}$, indicating that materials with the same $\phi_{Ny,b}$ and $\phi_{Ny,s}$ may be produced. However, we have no information on the blend surface morphology in this material. Elsewhere[28] we have discussed the possible surface morphologies that might be found in (bulk) phase-separated blends. Three possible extreme alternatives may be envisaged.

(1) Bulk morphology extending to the surface.
(2) Mixing of the two polymers in the surface region.
(3) Preferential adsorption of one of the polymers at the surface.

The data reported here strongly suggest that, in this system, there is a preferential overlayer of one polymer formed at the blend surface; however, at the point $\phi_{Ny,b}=0.55$ option 2 cannot be ruled out.

CONCLUSIONS

Mixtures of *m*-C and *o*-DCB may be used as a common solvent to prepare Ny-6/PB blends. Maximum (total) polymer solubility, with $\phi_{Ny,b}$ fixed at 0.32, was achieved at a solution composition of $X_{m\text{-}C}=0.4$. Solubility parameters do not predict correctly the observed experimental behaviour; specific directional and acid-based interactions played an important role in the dissolution of the polymers in this system.

Ny-6 can enrich the surface of the blends against the surface tension argument. The extent of enrichment depends on the polymer solution concentration, and to a much lesser extent, on the solvent composition employed. Increasing the polymer solution concentration favoured Ny-6 enrichment at the surface of the blends, but this enrichment did not show a concentration profile within the X.p.s. sampling depth. We argue that surface enrichment can be explained using the phase diagram in *Figure 1* and by considering how the blend composition changes with solvent extraction. For starting compositions safely within the one-phase region, higher polymer concentrations ensured that the precipitation of PB occurred first as a result of solvent removal (*o*-DCB being the lower-boiling-point solvent and the solvent for PB, which was also the higher-molecular-weight polymer). This result supports the proposition that, in this system,

the enrichment of the surface is due primarily to solvent–polymer interactions.

Molecular-weight effects play a role in determining blend surface composition. The LMWM in Ny-6, presumably monomer and cyclic oligomers, arising from 're-equilibration' of the polymer, manifest in the blend surface, leading to an over-estimation of the amount of surface enrichment. However, the concentration effect (described in ref. 1) was still observed when using purified nylon.

In the one-phase region ($X_{m\text{-}C}=0.3$–0.5), blend composition, i.e. $\phi_{Ny,b}$, also influences the extent of surface enrichment, but the effect of this parameter is secondary to both the solution concentration and any molecular-weight effect. The behaviour seen with Ny-6 at 5 and $10\,g\,l^{-1}$ is very different, indicating how polymer solution concentration dominates this parameter, and the true effect can only be seen in the purified Ny-6 blends. We make no attempt to explain how $\phi_{Ny,b}$ influences surface composition.

We conclude that, in the production of solution-cast blends, at least three parameters influence surface composition and that the final surface is determined by the parameter with the greatest influence, in this work, polymer–solvent interactions. The polymers are themselves immiscible and this was seen in the films, i.e. bulk phase separation was apparent. However, polymer A–polymer B interactions do not play such an important part in the control of surface composition, where blend 'history' is much more critical.

ACKNOWLEDGEMENTS

We would like to thank Professor Frank Jones for helpful discussions and guidance, and the Mexican National Council of Science and Technology (CONACyT) for the PhD grant for J. L. Angulo-Sanchez. We would also like to thank the referees who read the paper carefully and brought us up-to-date on the theory of interfacial segregation.

REFERENCES

1 Paul, D. R. and Newman, S. (Eds.) 'Polymer Blends', Vols I and II, Academic Press, New York, 1978
2 Coleman, M. M., Serman, C. J., Bhagwagar, D. E. and Painter, P. C. *Polymer* 1990, **31**, 1187
3 Borggreve, R. J. M., Gaymans, R. J., Schuijer, J. and Ingen Housz, J. F. *Polymer* 1987, **28**, 1489
4 Olabisi, O., Robeson, L. M. and Shaw, M. T. 'Polymer–Polymer Miscibility', Academic Press, New York, 1979
5 Clark, M. B., Jr, Burchardt, C. A. and Gardella, J. A., Jr *Macromolecules* 1991, **24**, 799
6 Bhatia, Q. S., Burrell, M. C. and Chera, J. J. *J. Appl. Polym. Sci.* 1992, **46**, 1915
7 P. Sakellariou, P. *Polymer* 1993, **34**, 3408
8 Hariharan, A., Kumar, S. K. and Russel , T. P. *Macromolecules* 1990, **23**, 3584
9 Hariharan, A., Kumar, S. K. and Russel, T. P. *Macromolecules* 1991, **24**, 4909
10 Hariharan, A., Kumar, S. K. and Russel, T. P. *J. Chem. Phys.* 1993, **98**(5), 4163
11 Brandrup, I. and Immergut, E. H. 'Polymer Handbook', 3rd Edn., Wiley, New York, 1989
12 Hansen, C. M. *Ind. Eng. Chem., Prod. Res. Dev.* 1969, **8**, 2
13 Hansen, C. M. and Skaarup, K. *J. Paint Technol.* 1967, **39**, 511
14 Coleman, M. M., Graf, J. F. and Painter, P. C. 'Specific Interactions and the Miscibility of Polymer Blends', Technomic, Lancaster, PA, 1991
15 Bonn, R. and van Aartsen, J. J. *Eur. Polym. J.* 1972, **8**, 1055
16 Theodorou, D. *Macromolecules* 1989, **22**, 4578
17 Lee, L. H. *Polym. Sci. (A-2)* 1967, **5**, 1103
18 Penn, L. S. and Bowler, E. R. *Surf. Interface Anal.* 1981, **3**(4), 161
19 Briggs, D. and Seah, M. P. 'Practical Surface Analysis', Wiley, Chichester, 1992
20 Clark, D. T. and Thomas, H. R. *J. Polym. Sci., Polym. Chem. Edn.* 1977, **15**, 2843
21 Andrews, J. M., Jones, F. R. and Semlyen, J. A. *Polymer* 1974, **15**, 420
22 Waters, Associates, 'Mark–Houwink Constants for PB'
23 Schuttenberg, V. H. and Schultz, R. C. *Angew. Chem.* 1976, **88**(24), 848
24 Chehimi, M. M., Watts, J. F., Jenkins, S. N. and Castle, J. E. *J. Mater. Chem.* 1992, **2**(2), 209
25 Fowkes, F. M. *J. Adhes. Sci. Technol.* 1987, **1**(1), 7
26 Wu, S. *Polym. Eng. Sci.* 1987, **28**, 1855
27 Tompa, H. 'Polymer Solutions', Butterworths, London, 1956
28 Short, R. D., Ameen, A. P., Jackson, S. T., O'Toole, L., Pawson, D. J. and Ward, A. J. *Vacuum* 1993, **44**(11/12), 1143